Experimental Studies of Instabilities and Confinement of Energetic Particles on JET and on MAST

S.E.Sharapov 1), B.Alper 1), F.Andersson 2), Yu.F.Baranov 1), H.L.Berk 3), L.Bertalot 4), D.Borba 5), C.Boswell 6), B.N.Breizman 3), R.Buttery 1), C.D.Challis 1), M.de Baar 7), P.de Vries 1), L.-G.Eriksson 8), A.Fasoli 9), R.Galvao 10,5), V.Goloborod'ko 11,12), M.P.Gryaznevich 1), R.J.Hastie 1), N.C.Hawkes 1), P.Helander 1), V.G.Kiptily 1), G.J.Kramer 13), P.J.Lomas 1), J.Mailloux 1), M.Mantsinen 14), R.Martin 1), F.Nabais 5), M. F. Nave 5), R.Nazikian 13), J-M.Noterdaeme 15), M.S.Pekker 3), S.D.Pinches 15), T.Pinfold 1), S.V.Popovichev 1), P.Sandquist 2), D.Stork 1), D.Testa 9), A.Tuccillo 4), I.Voitsekhovich 1), V.Yavorskij 11,12), N.P.Young 1), F.Zonca 4), JET-EFDA Contributors* and the MAST Team.

1. Euratom/UKAEA Fusion Assoc., Culham Science Centre, Abingdon, UK. **2.** Euratom/VR Fusion Assoc., Chalmers University of Technology, Goteborg, Sweden **3.** IFS, Univer. of Texas at Austin, Austin, USA **4.** Assoc. Euratom/ENEA/CNR Fusione, Frascati, Italy **5.** Euratom/IST Fusion Assoc., Centro de Fusao Nuclear, Lisboa, Portugal **6.** PSFC, Massachussets Institite of Technology, Cambridge, USA **7.** Assoc. Euratom-FOM Inst. Plasmaphys. 'Rijnhuizen', Nieuwegein, The Netherlands **8**. Assoc. Euratom/CEA, Cadarache, France **9**. CRPP/EPFL, Assoc. Euratom-Confederation Suisse, Lausanne, Switzerland **10**. Inst. Physics, University of Sao Paulo, Sao Paulo, Brazil **11.** Inst. Theor. Physics, Assoc. Euratom-OEAW, University of Innsbruck, Austria, **12**. Inst. Nuclear Research, Kiev, Ukraine **13**. Princeton Plasma Physics Laboratory, Princeton, USA **14**. Helsinki University of Technology, Assoc. Euratom-Tekes, Helsinki, Finland **15.** Max Planck Inst. Plasmaphysik, Euratom Assoc., Garching, Germany
e-mail contact of main author: sergei.sharapov@jet.uk

Abstract. In preparation for next step burning plasma such as ITER, experimental studies of instabilities and confinement of energetic ions were performed on JET and on MAST, with innovative diagnostic techniques, in conventional and shear-reversed plasmas, exploring a wide range of effects for energetic ions. "Alpha tail" production using 3rd harmonic ICRH of ^{4}He beam ions has been employed on JET for studying ^{4}He of the MeV energy range in a 'neutron-free' environment. The evolution of ICRH-accelerated ions of ^{4}He with E > 1.7 MeV and D with E>500 keV was assessed from nuclear gamma-ray emission born by the fast ions colliding with Be and C impurities. A simultaneous measurement of spatial profiles of fast ^{4}He and fast D ions relevant to ITER were performed and found to be in agreement with classical fast ion orbits in positive and strongly reversed magnetic shear discharges. Time-resolved gamma-ray diagnostics for ICRH-accelerated ^{3}He and H minority ions allowed changes in the fast ion distribution function to be assessed during sawteeth, TAEs, EAEs and Alfvén Cascades (ACs). A significant decrease of gamma-ray intensity from H ions with E>5 MeV was detected caused by the "tornado" modes (TAEs inside the q=1 surface); this was interpreted as TAE-induced loss of fast ions with drift orbit widths $\Delta_f \sim a/2$. Experiments performed in the opposite case, $\Delta_f/a \ll 1$, for ICRH-accelerated ^{3}He ions with E>500 keV, have shown excitation of numerous TAEs, EAEs, and ACs without a notable degradation of the fast ion confinement. Instabilities excited by super-Alfvénic beam ions were investigated on the spherical tokamak MAST. Due to higher values of beta and a higher proportion of fast ions on MAST than on JET, a wider variety of modes and nonlinear regimes for the Alfvén instabilities were observed. The MAST and START data showed that TAE and chirping modes decrease both in their mode amplitudes and in the number of unstable modes with increasing beta. Combining the JET and MAST results allows key parameter tests to be made and an integrated understanding of energetic particles to be developed.

1. Introduction

Losses and redistribution of fast ions due to magnetic field topology and fast ion driven instabilities such as Toroidal and Elliptical Alfvén Eigenmodes (TAEs and EAEs), Alfvén Cascades (ACs), and fishbones represent a serious concern for plasma heating, fast ion dynamics and transport in next-step burning plasma devices such as ITER [1]. ITER burning plasma will have several different groups of fast ions: α-particles, deuterium NBI in the MeV range and ICRH-accelerated ions (^{3}He and H). Therefore, simultaneous diagnosing of these fast ion populations will be necessary in order to establish possible loss channels and to identify the coupling between different groups of

* See Annex of J Pamela et al., this conference, paper OV/1-X

the fast ions and different fast-ion driven instabilities. These issues have been addressed in experiments on JET, with innovative diagnostic techniques, in conventional and shear-reversed plasmas, exploring a wide range of effects. A search for plasma conditions leading to a significant loss of energetic ions in both the prompt orbit/classical collision regime and in the presence of MHD perturbations was performed. In parallel, instabilities excited by super-Alfvénic fast ions were investigated in NBI-heated plasmas on the spherical tokamak MAST. Due to higher values of β and a higher ratio of $\beta_{fast}/\beta_{thermal}$ on MAST, a wider variety of modes and nonlinear regimes for the instabilities were observed [2].

2. Alpha-Simulation Experiments in Shear-Reversed Helium Plasmas

The ICRH 3rd-harmonic heating of ^{4}He beam ions was successfully used for accelerating ^{4}He up to T_{He}~1.1 ± 0.4 MeV energy and density of fast ^{4}He ions $n_{He}^{fast}/n_e \approx 10^{-3}$ in 'neutron-free' (neutron rate $R_n \leq 10^{14}$sec^{-1}) helium plasmas with monotonic $q(r)$-profiles [3]. The temperature and density of fast ^{4}He in these experiments were close to the obtained alpha-particle values in the record DT discharge #42976 on JET, T_α~ 1 MeV, $n_\alpha/n_e \approx 4{\cdot}10^{-3}$, with neutron rate, $R_n \approx 5.7{\cdot}10^{18}$ sec^{-1} [4]. In contrast to the real burning plasma, the ICRH discharges produce anisotropic distribution function of ^{4}He with fast profiles not determined by thermal ions as in burning plasma. Nevertheless, the 'alpha-production' technique [3] is useful for studying physics and developing diagnostics of fast ^{4}He in the MeV range, and it does not require an expensive DT operation. Here, we report on scenarios with strongly reversed magnetic shear and current holes (CH) [5, 6], which were among the priority considerations for validating the physics of fast ^{4}He ions as the confinement of alpha-particles has to be investigated thoroughly in such regimes [7, 8]. Development of reversed-shear scenarios compatible with alpha-production technique and measurements of fast ^{4}He ions were performed in these experiments.

Figure 1 shows the typical waveforms of high-power ICRH applied at 51 MHz in order to accelerate the low-power "seed" ^{4}He beam with energy 110 keV that efficiently couples to the RF-wave because of the beam particle finite Larmor radius. LHCD was applied during the inductive current ramp-up in order to obtain strong-reversed shear equilibrium. In the absence of the MSE measurements in these helium plasma and helium NBI discharges, MHD spectroscopy based on Alfvén Cascades (ACs) [9, 10] (Figure 2) and on strong-reversed-shear (SRS) sawteeth [11] was the main indicator of the shear-reversal. Spatial profiles of ^{4}He ions with energy >1.7 MeV were measured in discharges with monotonic (Fig. 3a) and non-monotonic (Fig. 3b) $q(r)$-profiles. These measurements were performed with 19-channel 2D camera detecting nuclear gamma-rays born in reaction ^{9}Be (^{4}He, nγ)^{12}C between ≈1.9 MeV ions of ^{4}He and Be impurity [12]. The measured profiles agree well with the topology of fast ion orbits in positive (banana-shape) and strongly reversed shear (vertical drift through the plasma centre) discharges in Figs. 4a and 4b correspondingly.

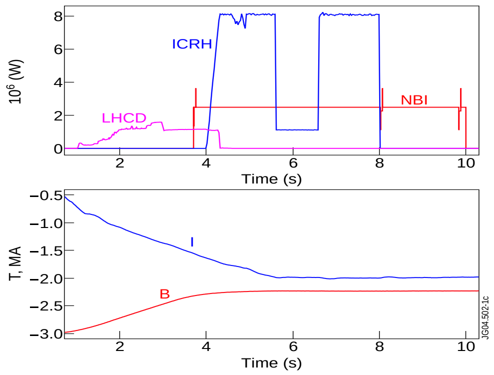

Fig.1 *Top: power waveforms of LHCD, ICRH, and ^{4}He NBI in JET discharge #63038. Bottom: inductive current and toroidal magnetic field.*

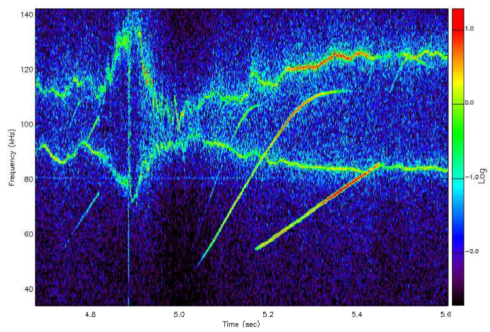

Fig.2 *Magnetic spectrogram showing Alfvén Cascades and SRS sawtooth (vertical line at t= 4.8 sec) in JET discharge #63038.*

Simultaneous measurements of spatial profiles of fast ^{4}He (Fig.3a) and fast D ions with E>500 keV (Fig. 3c) relevant to ITER were performed with the gamma-ray tomography for the first time.

This proof-of-principle measurement in a neutron-free environment encourages further development of the gamma-ray diagnostics for use in full-scale DT operation [13].

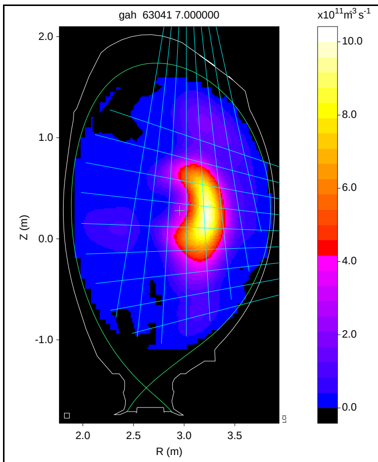

Fig.3a *Profile of gamma-ray emission from ⁴He ions in case of monotonic q(r)-profile*

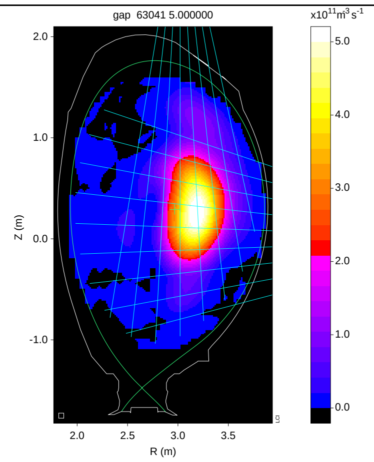

Fig.3b *Profile of gamma-ray emission from ⁴He ions in strongly reversed shear case*

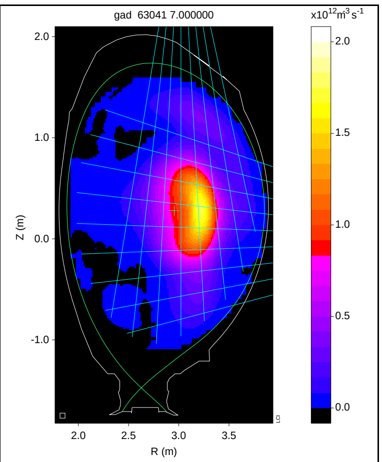

Fig.3c *Profile of gamma-ray emission from D ions in case of monotonic q(r)-profile*

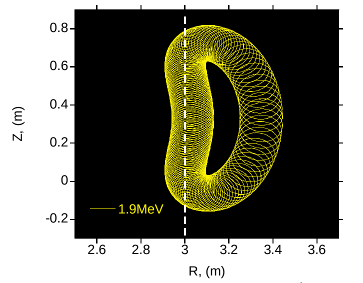

Fig.4a *ICRH-accelerated ⁴He ion orbit for Fig.3a.*

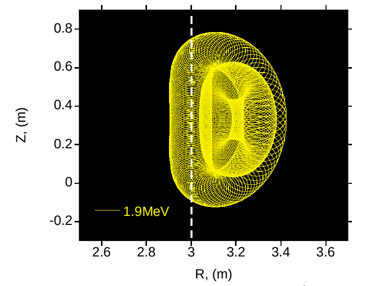

Fig.4b *ICRH-accelerated ⁴He ion orbit for Fig.3b.*

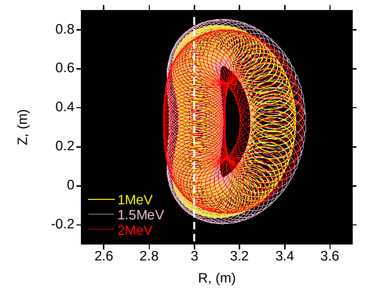

Fig.4c *ICRH-accelerated D ion orbits for Fig.3c.*

Experimentally, significant flux of escaping fast ⁴He ions was observed in the discharges in the form of severe hot spots seen as regions of bright visual light coming from the equatorial zone of poloidal limiters, about 20 cm in size. A scan of the plasma currents through the range $I_P^{\max}$ = 1.5÷2 MA (for B_0 = 2.2 T) was performed to determine the current needed to moderate fast ion losses. A tolerable level of the losses was found only at the highest current scanned, 2 MA. From this result one can infer that a low-current region/ current hole of radius up to $r_{CH} \approx 0.2\ a$ existed in these discharges thus re-normalising critical value of the total current as [8]

$$I_{crit}[MA] \cong \frac{0.55 \cdot I_{crit}^{mono}[MA]}{1-\sqrt{r_{CH}/a}} \cong \frac{1.4}{Z_i}\sqrt{\frac{\mu_i E[MeV]}{(R_0/a)}} \times \frac{1}{1-\sqrt{r_{CH}/a}}\,. \tag{1}$$

With the 2D gamma-ray tomography, it was also possible to observe an effect of sawtooth oscillations on the radial profile of ⁴He ions, for both the common $q=1$ sawteeth and the strong-reversed-shear (SRS) sawteeth. For the $q=1$ sawteeth, it was found that a transition from non-sawtoothing to sawtoothing plasma broadens the radial profile of the fast ions by ~5-10 cm. A tendency to a better confinement of fast ions has been observed after giant SRS sawteeth as Figures 5, 6 show. A giant SRS sawtooth observed at $t \approx 4.8$ sec was caused by a coupled instability associated with a simultaneous arrival of the magnetic surfaces $q=2$ at the centre and $q=4$ at the edge. It led to a transition from the strong-reversed-shear (current hole is likely) equilibrium to an equilibrium with weakly-reversed shear. Figure 6 shows that the gamma-ray emission had lower amplitude before the giant SRS sawtooth and increased significantly after SRS crash in line with expectations [7, 8].

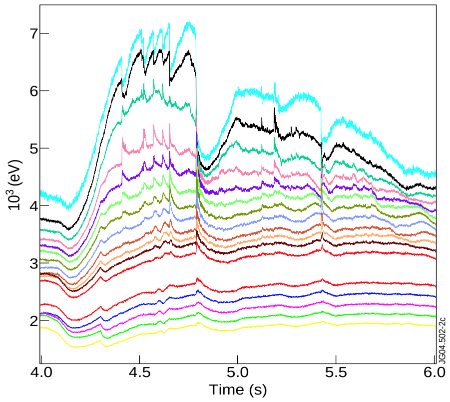

Fig.5 *T_e traces measured with multi-channel ECE at different radii in JET reversed-shear discharge #63041. Giant SRS sawtooth with drop $\Delta T_e / T_e \le 30\%$ is seen at t=4.8 sec.*

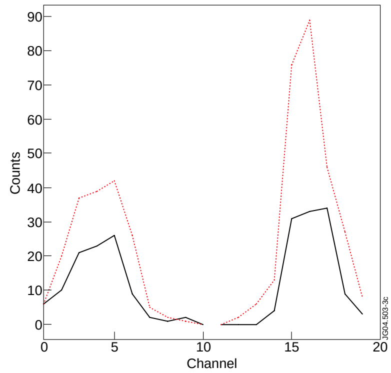

Fig.6 *Profiles of gamma-rays from fast ions before (solid) and after (dotted) SRS crash. Integration time 1 sec. Horizontal array: channel 1at top, channel 10 at bottom; vertical array: channel 11 at inner side of the torus and channel 19 at outer side*

3. TAE-induced Losses of ICRH-accelerated Protons with E>5 MeV on JET

Significant losses of ICRH-accelerated fast protons and degradation of total plasma energy content caused by the so-called “tornado” modes (TAE-modes localised within the $q = 1$ radius) were first detected on JT-60U and reported in [14]. The neutron counter was used in order to measure the time evolution of the fast protons with energy $E \ge 3$ MeV from the nuclear reaction ^{11}B(p,n)^{11}C. Modes similar to the tornado modes were then observed on DIII-D [15, 16] and on TFTR [17], and conclusions on significant loss of fast ions was drawn based on the observed loss of monster sawtooth stabilisation by the fast ions. More recently, tornado modes observed on JET were identified as core-localised TAEs [18], and the condition for their existence within the $q = 1$ radius, $r(q = 1)/R_0 < S$, where S is magnetic shear, was identified [19]. A significant (by a factor of two) decrease of gamma-ray emission coming from the nuclear reaction ^{12}C(p, p’γ)^{12}C, where the protons were accelerated with ICRH minority heating up to the energy range >5 MeV, were detected on JET during tornado and TAE mode activity. Figure 7 shows a sudden and significant decrease of the total intensity of the gamma-rays observed in a discharge with B_0 = 2.7 T, $I_P \approx 2$ MA, at $t \approx 10.5$ sec and $t \approx 12$ sec. The degradation of the gamma-ray intensity starts during a sawtooth-free period at steady-state ICRF heating, about 0.5 ÷ 1 sec before monster sawtooth crashes seen in Figure 8. It correlates in time with tornado modes and TAEs detected with external magnetic pick-up coils as Figures 9 and 10 show, which are the most likely explanation for the degradation of the proton-induced gamma-ray emission. Two different sets of modes in Figs. 9, 10 are TAEs with nearly constant frequencies and tornado modes with frequencies sweeping down as $q(0)$ decreases.

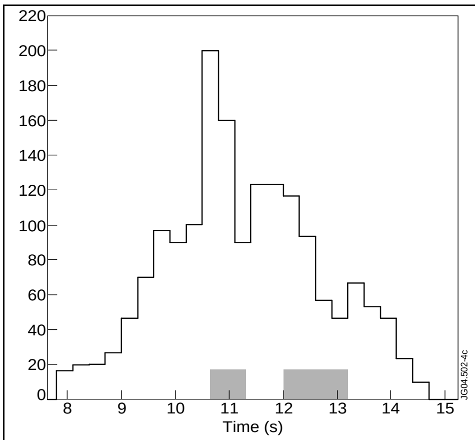

Fig.7 *Intensity of γ-rays born in nuclear reactions between fast H and C as measured with vertical γ-ray spectrometer in JET plasma. Shaded areas mark gamma-degradation periods.*

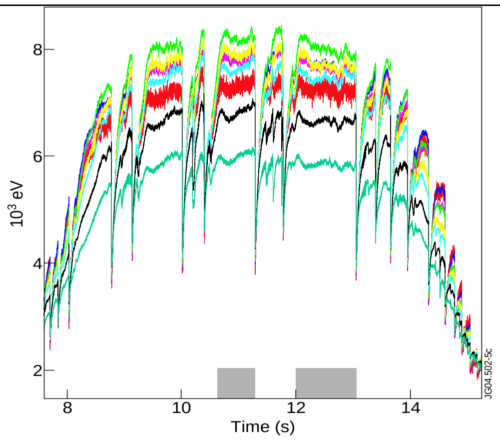

Fig.8 *Electron temperaturse measured by multi-channel ECE at different radii. Monster sawteeth at t=11.4 and t=13 s occur **after** degradation of gamma- intensity marked as shaded time intervals.*

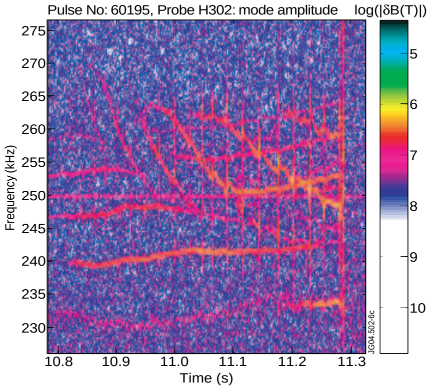

Fig.9 Magnetic spectrogram showing amplitude of TAEs & tornadoes as function of time and frequency (first shaded time interval in Fig.7).

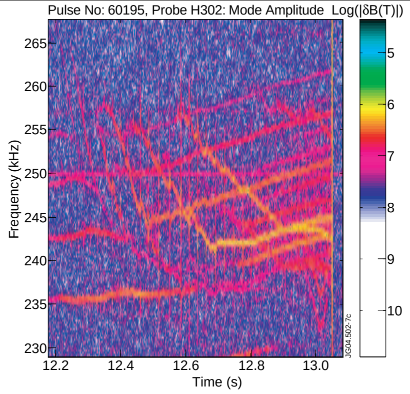

Fig.10 Magnetic spectrogram showing amplitude of TAEs & tornadoes as function of time and frequency (second shaded time interval in Fig.7).

Analysis of the Alfvén Eigenmode spectrum in the reconstructed equilibrium was performed with the ideal MHD MISHKA code [20]. It shows that the combination of the TAEs inside the $q=1$ radius (tornado) and outside the $q=1$ radius form a TAE-"corridor" that spreads from the central to a half-radius of the plasma as shown in Figure 11. Prompt losses of the trapped protons with $E>5$ MeV with orbit width up to $\Delta_f/a \le 0.5$ (Figure 12) significantly enhanced by the TAEs are considered as a primary channel of the proton losses in this case.

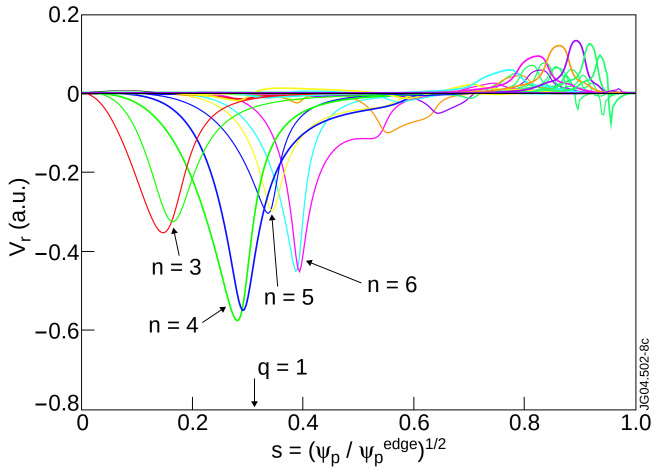

Fig.11. Core-localised TAEs with n=3, 4 and eigenfunctions within q=1 radius (tornado), and n=5,6 TAEs outside q=1 computed for JET equilibrium in #60195 at t=13 sec.

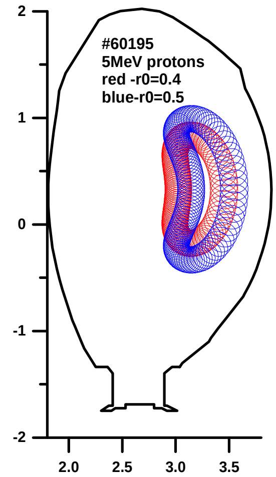

Fig.12. Orbits of 5 MeV protons accelerated with on-axis ICRH in JET discharge #60195.

4. Time-resolved measurements of ICRH-accelerated ^{3}He ions with E>500 keV on JET

In order to study a coupling between energetic ions and Alfvén Eigenmodes in the regime of smaller drift orbits of fast ions, $\Delta_f/a \approx 0.1 << 1$, which is more relevant for a larger-scale ITER-type machines, JET developed a scenario for Alfvén Eigenmodes excited with ICRF-accelerated ^{3}He minority in ^{4}He plasma. Fast ^{3}He ions with energy as low as 500 keV can interact with C and Be impurities and generate gamma-rays through nuclear reactions much more numerous than ^{4}He [12, 13]. Due to the high intensity of this gamma-ray emission from ^{3}He, time-resolved measurements of fast ^{3}He become possible. The choice of helium instead of deuterium was determined by two main reasons. First, for similar ion temperatures, ^{4}He thermal ions have lower speed than deuterium thermal ions, so that the ion Landau damping of AEs due to the $V_{\|i} = V_A/3$ resonance is exponentially smaller for AEs in ^{4}He plasma. Second, the low level of neutrons makes the gamma-ray measurements nearly free of the neutron noise, so a better quality gamma-ray images of the fast ^{3}He ions with time resolution up to 10 msec, could be obtained.

Figure 13 shows simultaneous measurements of the AE activity in the frequency range up to 450 kHz with Mirnov coil, together with the intensity of gamma-ray emission measured by the vertical gamma-ray camera in JET helium discharge #63099. In this discharge, magnetic field and maximum plasma current were $B = 3.3$ T, $I = 2.3$ MA correspondingly, electron temperature and density were $T_e(0) \approx 6.5$ keV, $n_e(0) \approx 2.5 \cdot 10^{19}$ m^{-3}, and the plasma composition was ^{4}He:D = 91:9. LHCD power of 1.7 MW was applied during the current ramp-up phase in order to obtain a reversed shear magnetic configuration, and ICRH power of 5 MW was applied for the on-axis heating of ^{3}He minority ions. Notches in the ICRH power from 5 MW down to 1 MW were performed in this discharge in order to observe both the decay and increase of the ^{3}He fast ion population with E > 500 keV on the gamma-ray diagnostics. It is seen in Figure 13 that numerous Alfvén Eigenmodes of different types were excited in this discharge: Alfvén Cascades, TAEs, and EAEs. Even more numerous AEs (not shown here) with higher mode numbers n were detected with the newly developed interferometry technique [21]. It is seen that the notches in ICRH power affect significantly both the gamma-ray emission from ^{3}He ions, and the AEs, but different AEs are affected somewhat differently. Figure 14 shows that a sharp decrease in intensity of gamma-ray emission from ^{3}He with E > 500 keV is well correlated with the disappearance of the TAE modes. However, the Alfvén Cascades persist during the time of the notch in ICRH power, when no ^{3}He ions are detected with the gamma-ray camera. This indicates that the AC instability is caused by ^{3}He ions with energies lower than 500 keV, in correspondence with the observation of NBI-driven ACs on JET and on DIII-D [22]. In spite of the high amplitude AE activity in the whole frequency range covered by the MHD diagnostics, the time-resolved measurements of ^{3}He with E > 500 keV detected no notable degradation of gamma-ray emission due to any of the AEs observed in these discharges with the orbit widths $\Delta_f / a << 1$.

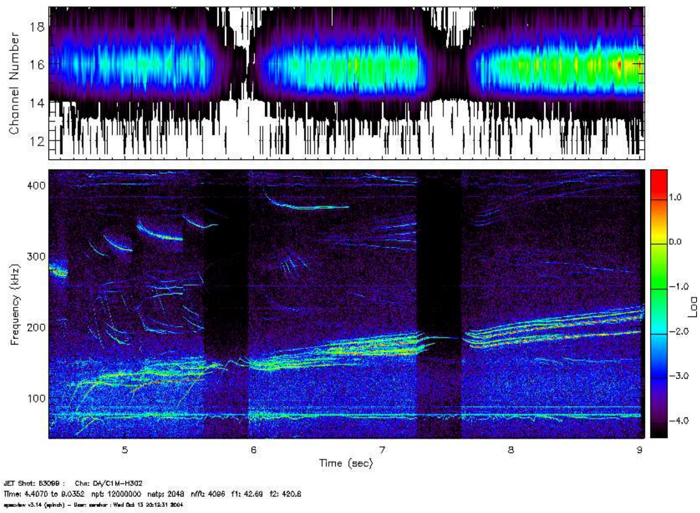

Fig.13 *Top: intensity of γ-rays born in nuclear reactions between fast ^{3}He and Be as measured with vertical γ-ray camera (channel 11 is at the inner side of the torus and channel 19 at the outer side). Bottom: Magnetic spectrogram showing Alfvén Cascades, TAEs and EAEs excited by fast ^{3}He ions at the time of measurements of the ^{3}He profile (discharge #63099).*

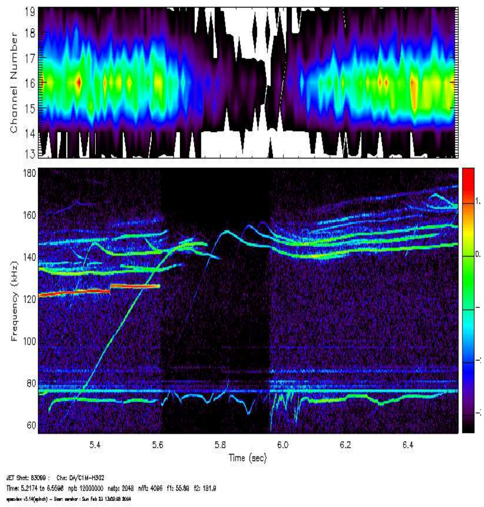

Fig.14 *Zoom of Figure 13: Top: intensity of γ-rays born in nuclear reactions between fast ^{3}He and Be. Bottom: Magnetic spectrogram showing Alfvén Cascades and TAEs excited by fast ^{3}He ions.*

5. Grassy Sawteeth in Low-Density JET Discharges

Fast particles play a major role in the $q = 1$ sawtooth stabilisation, and the effect of alpha-particles on sawteeth in burning plasma is one of the most important problems of burning plasma [23]. It was discovered some time ago on JET that in plasmas of low density, $n_e \leq n_e^{crit} \approx 2 \times 10^{19}$ m^{-3}, with high-power ICRF-heating the ICRH-accelerated ions fail to stabilise sawteeth even though the fast ion energy content could be comparable to that of thermal plasma [24]. With plasma density decreasing, discharges abruptly change from the usual monster sawtooth regime to a regime with very short period and more chaotic “grassy” sawteeth as soon as the threshold in density is passed. These grassy sawteeth are accompanied by higher-frequency activity, an $n = 1$ fishbone-like modes [25, 26] and AEs. Possible explanations for the loss of fast ion stabilising effect were searched for and the orbit width of the fast ions exceeding the $q = 1$ radius [26] and possible generation of supra-thermal electrons during sawtooth crashes similar to [27] were identified as the main density-dependent effects. In order to investigate these effects, dedicated experiments were performed in JET low-density plasmas with high power, $P > 4$ MW, ICRF-heating of hydrogen minority ions. The effect of fast ion profiles on sawteeth was studied with on- and off-axis ICRH and with ICRH launched co- and counter-current. Figures 15 (a-c) show typical time traces of electron temperature in JET discharges with ICRF hydrogen minority heating with (a) dipole; (b) +90^0 phasing of the ICRH antenna, and (c) –90^0 phasing. The wave with +90^0 phasing corresponds to the co-current direction and it generates a more peaked radial profile of fast ions with higher temperature [28, 29]), while the wave launched in the counter-current direction (-90^0) produces a flattish radial profile of the fast ions with lower temperature. In all three cases sawteeth with periods shorter than monster sawtooth period were obtained, in spite of the different radial profiles and temperatures of fast ions. However, these three cases show a distinctly different behaviour of the cold kink perturbation (seen as oscillatory structure), and cannot be counted as a single grassy sawtooth phenomenon and should be studied separately.

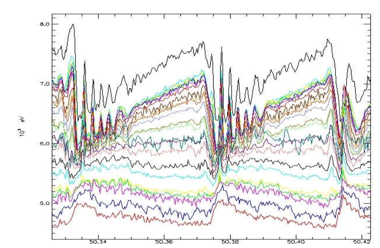

Fig. 15 (a) T_e measured with ECE in JET discharge #62465.

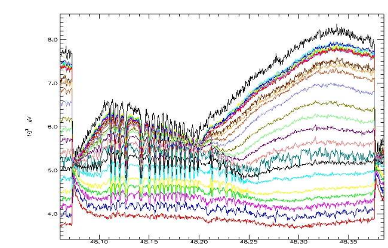

Fig. 15 (b) T_e measured with ECE in #62478 (+90^0 ICRH phasing)

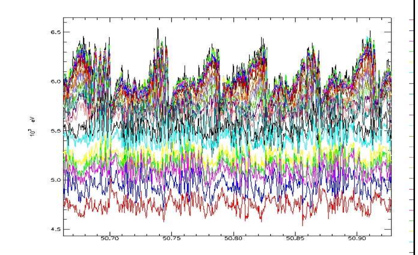

Fig. 15 (c) T_e measured with ECE in #62478 (-90^0 ICRH phasing)

Measurements of supra-thermal electron emission in the energy range from 150 keV to 450 keV were made with Fast Electron Bremsstrahlung camera with the lines-of-sight through the central region of the plasma at 90^0 angle with respect to the magnetic axis. These measurements show a significant increase of the suprathermal electron emission throughout the monster sawtooth phase and just before the transition from grassy to monster sawteeth. This emission is not observed in the grassy sawtooth regime. Bursts of supra-thermal ECE emission is also seen during the monster sawtooth crashes. Estimates show that in these low-density high-temperature discharges the electric field was close to the critical field for the runaway electrons, $E \approx E_{crit}$, so the sawtooth crashes could affect the runaways by generating electric field comparable to the near-threshold value $E_{crit} - E$. The observations above underline the problem of what role supra-thermal electrons play in sawteeth.

6. Alfvén Eigenmodes in High-β Spherical Tokamaks

Very important data on fast ion-driven modes has been obtained on the spherical tokamaks MAST and START. The low toroidal magnetic field, $B < 0.5$ T, of the STs makes these machines a perfect test bed for studying energetic particle driven modes due to the super-Alfvénic nature of NBI at energy as low as 30 keV [2]. Lots of Alfvén instabilities excited by NBI-produced energetic ions have been observed on START and MAST: fixed-frequency modes in the TAE and EAE frequency ranges, frequency-sweeping “chirping” modes, fishbones, and modes at frequencies above the AE frequency range. The key ratio that determines the perturbative versus non-perturbative type of the mode $\beta_{fast} / \beta_{thermal}$ in STs can be higher than that usually obtained in other tokamaks. The record value of volume-averaged $\beta \cong 40\%$, achieved in START NBI-heated plasmas and the concept of high-β burning plasma STs being considered [30] makes it necessary to re-consider the role of thermal and fast ions in the electromagnetic instabilities. The problem of a dominant fast ion driven instability at high-β was assessed on MAST experimentally and a similar analysis of earlier data from START was performed. The data shows that the two major pressure-gradient driven fast ion instabilities, TAEs and chirping modes decrease both in mode amplitudes and in the number of unstable modes with increasing β. On START, the chirping mode amplitude decreases as β increases as Figure 16 shows. Chirping modes disappear as β increases and they have not been observed in high-β discharges. The initial increase of the mode amplitude with β-increase is caused by the increase in the fast ion pressure. Figure 17 shows that a similar tendency to the chirping mode disappearance at higher β is observed on MAST. The importance of fast-ion driven instabilities in burning plasma spherical tokamaks, which would necessarily operate in high-beta regimes, has to be investigated both experimentally and theoretically although it is expected that many of the numerous energetic-particle-driven instabilities observed at low-beta in present-day machines will be absent in the higher-beta burning plasma devices.

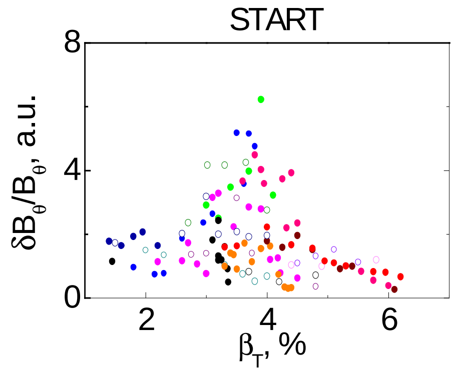

***Fig.16**. On START, the chirping mode amplitude decreases as beta increases.*

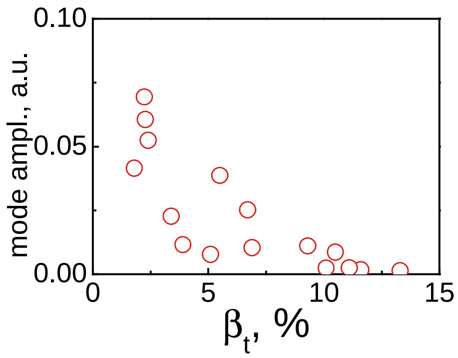

***Fig.17** Dependence on β of the maximum amplitude in a single burst of chirping modes, in NBI discharges on MAST.*

This work was performed under the European Fusion Development Agreement and was partly funded by Euratom and the UK Engineering and Physical Sciences Research Council.

[1] ITER Physics Basis, Nuclear Fusion **39** (1999) 2137
[2] GRYAZNEVICH M.P. and SHARAPOV S.E. Plasma Phys. Control. Fusion **46** (2004) S15
[3] MANTSINEN M et al., Phys. Rev. Lett. **88** (2002) 105002
[4] KEILHACKER, M., Phil. Trans. R. Soc. London A **357** (1999) 415
[5] HAWKES N et al., Phys. Rev. Lett. **87** (2001) 115001
[6] FUJITA T et al., Phys. Rev. Lett. **87** (2001) 245001
[7] YAVORSIJ V et al., Nuclear Fusion **43** (2003) 1077
[8] YAVORSIJ V et al., Nuclear Fusion **44** (2004) L5
[9] SHARAPOV S.E. et al., Phys. Letters **A289** (2001) 127
[10] BERK H.L. et al., Phys. Rev. Lett. **87** (2001) 185002
[11] CHALLIS C.D. et al., Plasma Phys. Control Fusion **43** (2001) 861
[12] KIPTILY V. G. et al., Nuclear Fusion **42** (2002) 999
[13] KIPTILY V. G. et al, to be submitted to Phys. Rev. Lett. (2004)
[14] SAIGUSA M., et al., Plasma Phys. Control. Fusion **40** (1998) 1647
[15] HEIDBRINK W.W. et al., Nuclear Fusion **39** (1999) 1369
[16] BERNABEI S. et al., Nuclear Fusion **41** (2001) 513
[17] BERNABEI S. et al., Phys. Rev. Lett. **84** (2000) 1212
[18] BERK H.L. et al., Phys. Plasmas **2** (1995) 3401
[19] KRAMER G.J. et al., Phys. Rev. Lett. **92** (2004) 015001
[20] MIKHAILOVSKII A.B. et al., Plasma Phys. Reports **23** (1997) 844
[21] SHARAPOV S.E. et al., Phys. Rev. Lett. **93** (2004) 165001
[22] NAZIKIAN R. et al., this conference, EX/5-1 (2004)
[23] PORCELLI F. et al., Phys. Plasmas **3** (1994) 470
[24] MANTSINEN M. et al., Plasma Phys. Control. Fusion **42** (2000) 1291
[25] GORELENKOV N.N. et al., this conference TH/5-2Rb (2004)
[26] NABAIS F. et al, this conference TH/5-3 (2004)
[27] SAVRUKHIN P.V. Phys. Rev. Lett. **86** (2001) 3036
[28] ERIKSSON L.-G. et al., Phys. Rev. Lett. **81** (1998) 1231
[29] MANTSINEN M. et al., Phys. Rev. **89** (2002) 115004
[30] WILSON H., et al., this conference FT/3-1Ra (2004)